Electronic Supplementary Material (ESI) for RSC Advances.

# Supporting Information

## Polycrystalline iron oxide nanoparticles prepared by C-dots-mediated aggregation and reduction for supercapacitor application

*Dejian Chen, Shunxing Li,* Biyan Xu, Fengying Zheng, Haifeng Zhou, Huiwu Yu, Fan Lin and Xiaoqi Zhu*

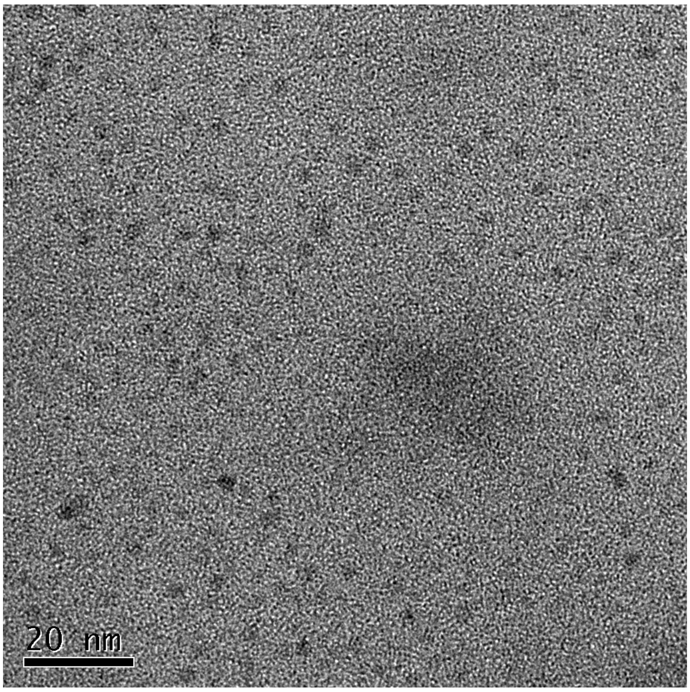

**Figure S1.** Typical TEM image of carbon dots.

The evolution of the morphology of carbon dots was illustrated by transmission electron microscopy (TEM). TEM images in Figure S1 clearly revealed that a uniform dispersion of the C-dots in water with the average diameter of 3 nm.

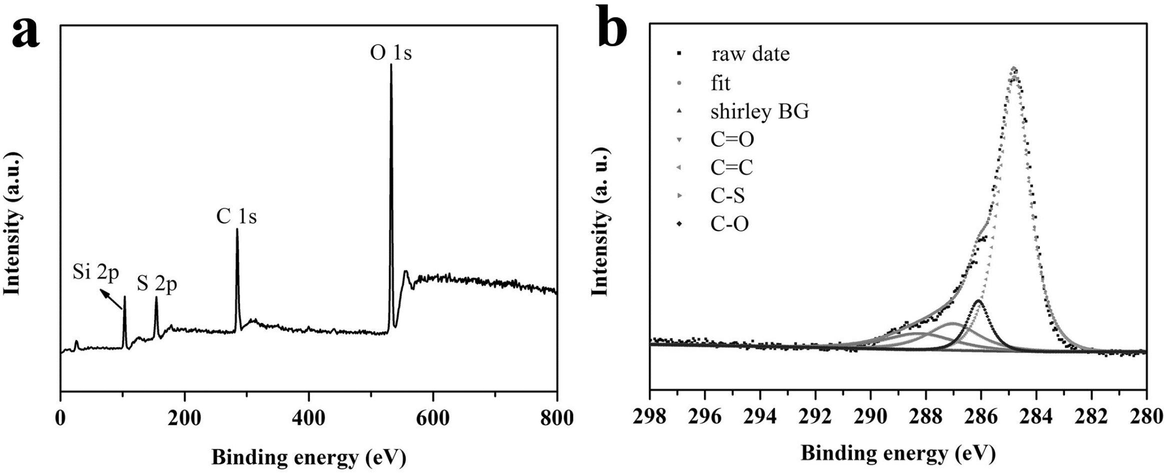

**Figure S2. (a)** The XPS survey spectrum and (b) C 1s of carbon dots.

X-ray photoelectron spectroscopy (XPS) was used to further investigate the chemical nature of the atoms in the C-dots. The XPS survey spectrum in Figure S2a showed the $S_{2p}$, $C_{1s}$, and $O_{1s}$ at a binding energy of 159.2 eV, 284.8 eV and 532.8 eV, respectively. The high-resolution XPS $C_{1s}$ spectrum of the C-dots (Figure S2b) was asymmetric because of the presence of C-C and C=C bonds as well as heteroatom bonds. The multicomponent analysis of the C1s line confirmed the presence of C-S (287.0 eV), C-C/C=C (284.8 eV), as well as that of several oxygen contained functional groups, such as C-O (286.1 eV), and C=O (288.2 eV) bonding moieties.

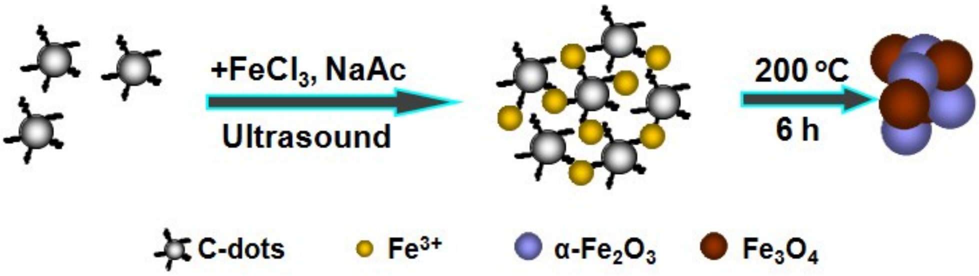

**Figure S3.** The construction of α-$Fe_2O_3$/$Fe_3O_4$ heterostructured nanoparticles.

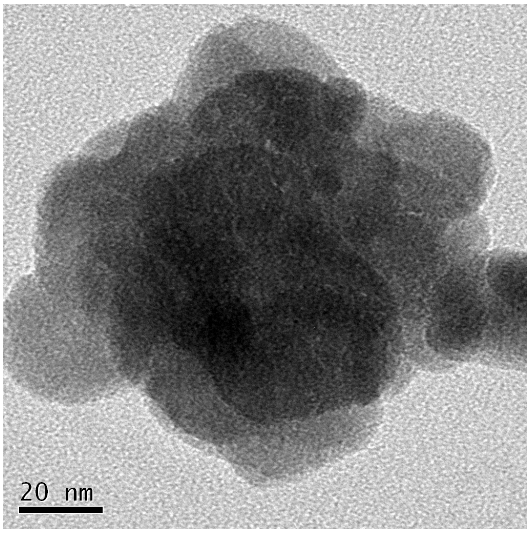

**Figure S4**. TEM image of α-$Fe_2O_3$/$Fe_3O_4$ heterostructured nanoparticles.

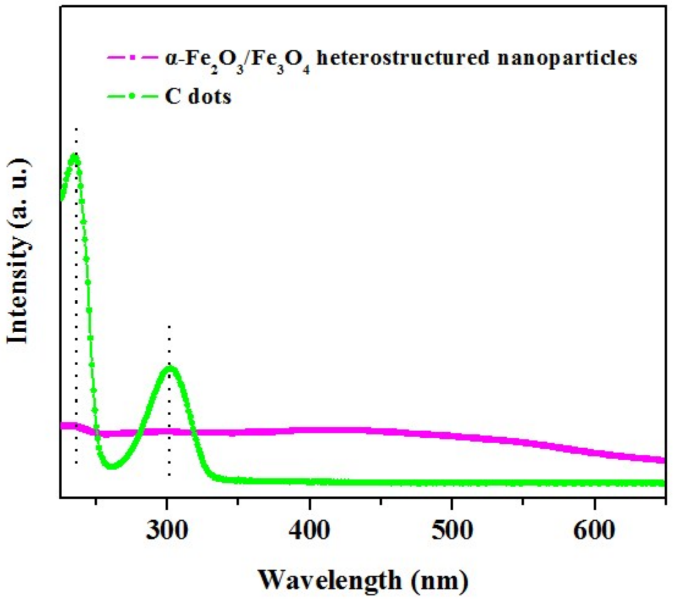

**Figure S5**. UV-Vis spectra ofα-$Fe_2O_3/Fe_3O_4$ heterostructured nanoparticles.

The forming mechanism of $Fe_2O_3/Fe_3O_4$ nanoparticles mediated by C-dots was confirmed by the spectrum data of **Fig. S5**. In the UV-Vis spectrum, two peaks around 220 and 300 nm were observed, which revealed the successful formation of a hybrid materials with C-dots and iron oxide. C-dots-mediated aggregation and reduction were important for the control the morphology, structure, and function of iron oxide particles.

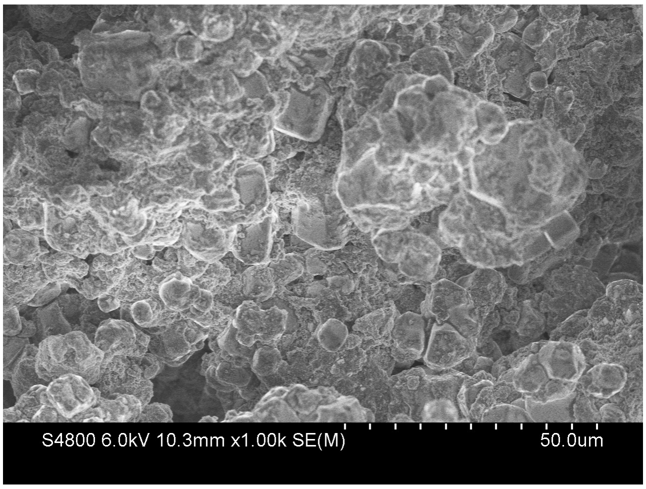

**Figure S6.** SEM image of particles without using C-dots in the hydrothermal synthesis.

Figure S6. showed the SEM image of particles without using C-dots in the hydrothermal synthesis, it can seen that the particles are micron sizes with ruleless morphology.

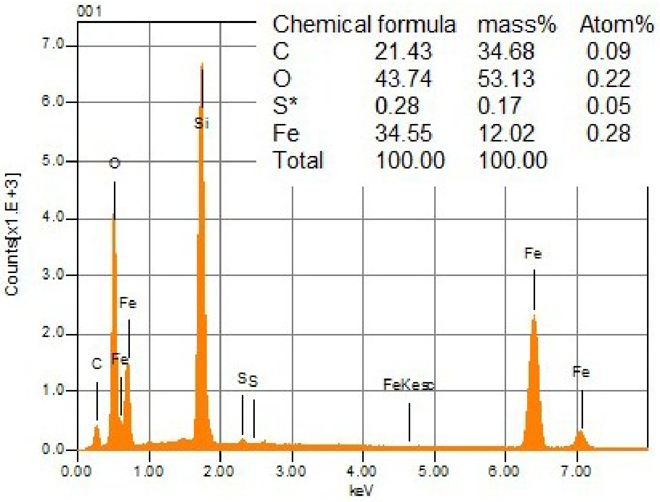

| Chemical formula | | mass% | Atom% |
|---|---|---|---|
| C | 21.43 | 34.68 | 0.09 |
| O | 43.74 | 53.13 | 0.22 |
| S* | 0.28 | 0.17 | 0.05 |
| Fe | 34.55 | 12.02 | 0.28 |
| Total | 100.00 | 100.00 | |

**Figure S7.** EDS image at the selected-area of heterostructure α-$Fe_2O_3$/$Fe_3O_4$ nanoparticles.

The EDS showed in Figure S7 indicated that heterostructure α-$Fe_2O_3$/$Fe_3O_4$ nanoparticles were mainly contained Fe and O elements, the C and S element were few.

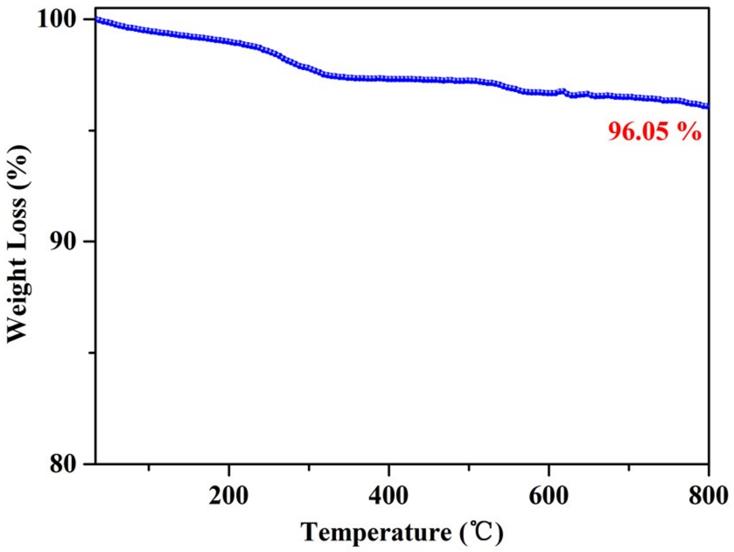

**Figure S8.** Thermogravimetric (TG) curves of heterostructure α-$Fe_2O_3$/$Fe_3O_4$ nanoparticles. The TG curves were obtained in $N_2$ with a heating rate of 5 °C/min.

TGA measures the weight loss with respect to temperature under controlled environment. The C-dots were stable at 110 °C and loss their weight at about 450 °C. The amount of C dots in the heterostructure α-$Fe_2O_3$/$Fe_3O_4$ nanoparticles was trace (about 2.1 %). The amount of materials used in electrode was at mg level, so we not considered in the weight of electrodeactive materials.

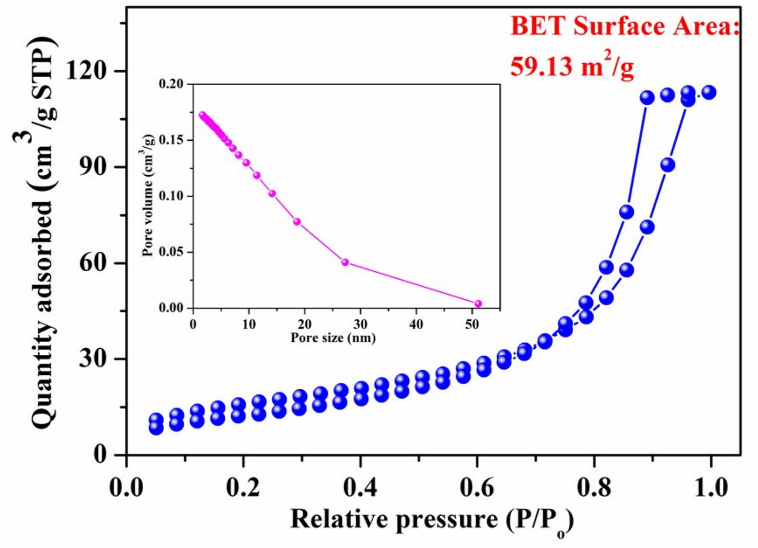

**Figure S9.** Nitrogen adsorption-desorption isotherms of heterostructure α-$Fe_2O_3/Fe_3O_4$ nanoparticles. Inset is pore distribution curve.

A typical type IV curve at low relative pressure and a hysteresis loop, could be observed, indicating the presence of complex pore structure, and the pore size and pore volume were shown in the insert of **Fig S9**. The BET surface area of as-prepared α-$Fe_2O_3/Fe_3O_4$ nanoparticles was 59.13 m$^2$ g$^{-1}$.

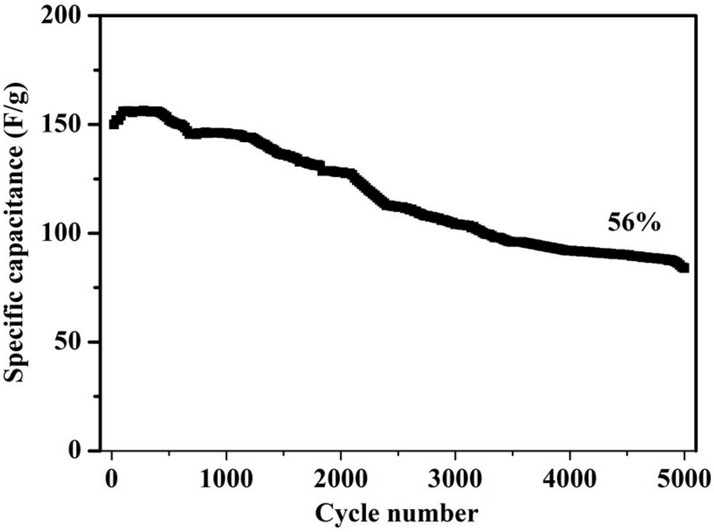

**Figure S10.** Cycling performance of heterostructure $\alpha$-$Fe_2O_3/Fe_3O_4$ nanoparticles as anodic electrode materials that measured at 1 A $g^{-1}$.

The heterostructure $\alpha$-$Fe_2O_3/Fe_3O_4$ nanoparticles anodic electrode showed superior long-term electrochemical stability with cycling efficiency of 56 % after 5000 cycles.

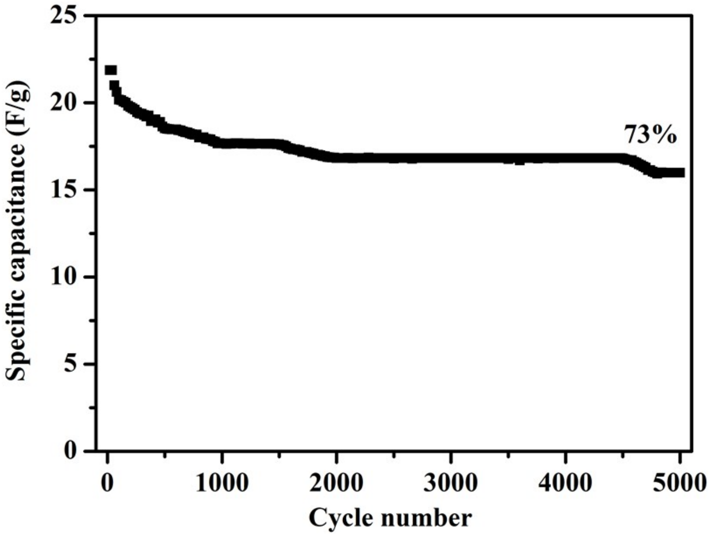

**Figure S11.** Cycling performance of heterostructure α-$Fe_2O_3$/$Fe_3O_4$ nanoparticles as cathodic electrode materials that measured at 1 A $g^{-1}$.

The heterostructure α-$Fe_2O_3$/$Fe_3O_4$ nanoparticles cathodic electrode showed superior long-term electrochemical stability with cycling efficiency of 73 % after 5000 cycles.